Resolution of a chronic viral infection after interleukin-10 receptor blockade

Mette Ejrnaes,[1] Christophe M. Filippi,[1] Marianne M. Martinic,[1] Eleanor M. Ling,[1] Lisa M. Togher,[1] Shane Crotty,[2] and Matthias G. von Herrath[1]

[1]Immune Regulation Lab – DI3 and [2]Division of Vaccine Discovery, La Jolla Institute for Allergy and Immunology, La Jolla, CA 92037

A defining characteristic of persistent viral infections is the loss and functional inactivation of antiviral effector T cells, which prevents viral clearance. Interleukin-10 (IL-10) suppresses cellular immune responses by modulating the function of T cells and antigen-presenting cells. In this paper, we report that IL-10 production is drastically increased in mice persistently infected with lymphocytic choriomeningitis virus. In vivo blockade of the IL-10 receptor (IL-10R) with a neutralizing antibody resulted in rapid resolution of the persistent infection. IL-10 secretion was diminished and interferon γ production by antiviral CD8^{+} T cells was enhanced. In persistently infected mice, CD8α^{+} dendritic cell (DC) numbers declined early after infection, whereas CD8α^{−} DC numbers were not affected. CD8α[−] DCs supported IL-10 production and subsequent dampening of antiviral T cell responses. Therapeutic IL-10R blockade broke the cycle of IL-10–mediated immune suppression, preventing IL-10 priming by CD8α[−] DCs and enhancing antiviral responses and thereby resolving infection without causing immunopathology.

CORRESPONDENCE
Matthias G. von Herrath:
matthias@liai.org

Abbreviations used: BFA, Brefeldin A; HCV, hepatitis C virus; LCMV, lymphocytic choriomeningitis virus; PD-1, programmed death 1 receptor; TLR, Toll-like receptor.

IL-10 inhibits a broad spectrum of cellular immune responses. It suppresses the function of APCs and T cells by inhibiting proinflammatory cytokine production, co-stimulation, MHC class II expression, and chemokine secretion (1, 2). IL-10 has been associated with immunopathology in various immune-mediated and inflammatory diseases. For example, treatment with a combination of anti–IL-10R monoclonal antibody and Toll-like receptor 9 (TLR9) ligands had potent therapeutic antitumor effects (3, 4), indicating a role for IL-10 in the pathogenesis of cancer.

Viruses use a variety of strategies to avoid recognition by the host immune system (5–7). The active induction of immune suppression is one mechanism by which viruses escape clearance and thus establish a persistent infection (8). In humans, chronic viral infections afflict millions of people worldwide (9–11). Interestingly, elevated levels of IL-10 production have been associated with persistent infection by hepatitis C virus (HCV) (12, 13), HIV (14–18), and Epstein-Barr virus (1, 19). It was recently reported that upon HCV infection, intrahepatic CD8^{+} T cells from persis-

tently infected subjects suppressed the in vitro proliferative responses of liver-derived lymphocytes in an HCV-specific and IL-10–dependent manner (20). Moreover, both CD4^{+} and CD8^{+} T cells have been shown to express high levels of IL-10 in HIV-infected individuals (14, 15). In addition, a higher frequency of IL-10–producing CD4^{+} T cells was observed in HIV-infected individuals with progressive disease or active HIV replication compared with individuals in the latent phase of disease (16–18).

To gain further insight into the role of IL-10 in the establishment and maintenance of persistent viral infections, we investigated whether this cytokine is involved in the persistence of lymphocytic choriomeningitis virus (LCMV) infection in its natural host, the mouse. LCMV is an arena virus that can cause either acute or persistent infection in vivo depending on the strain, route of infection, and dose of virus (21). Although adult mice infected with LCMV Armstrong rapidly clear the infection and establish a stable memory T cell pool (22–27), infection with a naturally selected isolate of LCMV Armstrong, the LCMV variant clone 13, results in a prolonged infection that persists (28–30). This chronic infection is associated with the functional impairment, exhaustion,

M. Ejrnaes, C.M. Filippi, and M.M. Martinic contributed equally to this paper.

and deletion of virus-specific CD8^{+} T cells (31, 32), resulting in viral persistence, which was recently linked to expression of the programmed death 1 receptor (PD-1), an inhibitory receptor of the CD28 family (33–36).

DCs, which are key regulators of immune responses, play an important role in clearing viral infections. Upon engagement of DCs, naive Th cells polarize into IFN-γ–producing Th1 or IL-4–producing Th2 effector cells (37, 38). It has previously been suggested that different DC subsets, for example CD11c^{+}CD8α^{−} and CD11c^{−}CD8α^{+} DCs, have the potential to differentially induce Th2 and Th1 cells, respectively (39–41). Others have previously reported that, after LCMV clone 13 infection, LCMV-specific CD4^{+} T cells from TCR transgenic SMARTA mice produced higher levels of IL-10 than after LCMV Armstrong infection (42). In this study, we demonstrate that production of IL-10 during LCMV clone 13 infection is associated with viral persistence, because blockade of the receptor for IL-10 restored the antiviral immune response and resulted in viral clearance. This rapid resolution of viral infection after anti–IL-10R treatment was associated with diminished levels of endogenous IL-10 production and enhanced antiviral CD8^{+} T cell responses. Further analysis revealed that viral persistence during LCMV clone 13 infection was linked to a decline in the number of CD11c^{+}CD8α^{+} DCs.

CD11c^{+}CD8α^{−} DCs efficiently induced IL-10 secretion by antiviral CD4^{+} T cells, preventing viral clearance and therefore enabling viral persistence. Therapeutic IL-10R blockade broke the cycle of IL-10–mediated immune suppression, preventing IL-10 priming by CD8α[−] DCs and enhancing antiviral responses, thereby resolving infection in persistently infected mice.

These results highlight for the first time the role of IL-10 in the suppression of an antiviral immune response during a persistent viral infection. Upon blockade of signaling through the IL-10R, secretion of IL-10 was almost completely abrogated. We therefore propose that IL-10R blockade may be of therapeutic benefit in the treatment of chronic viral infections.

RESULTS

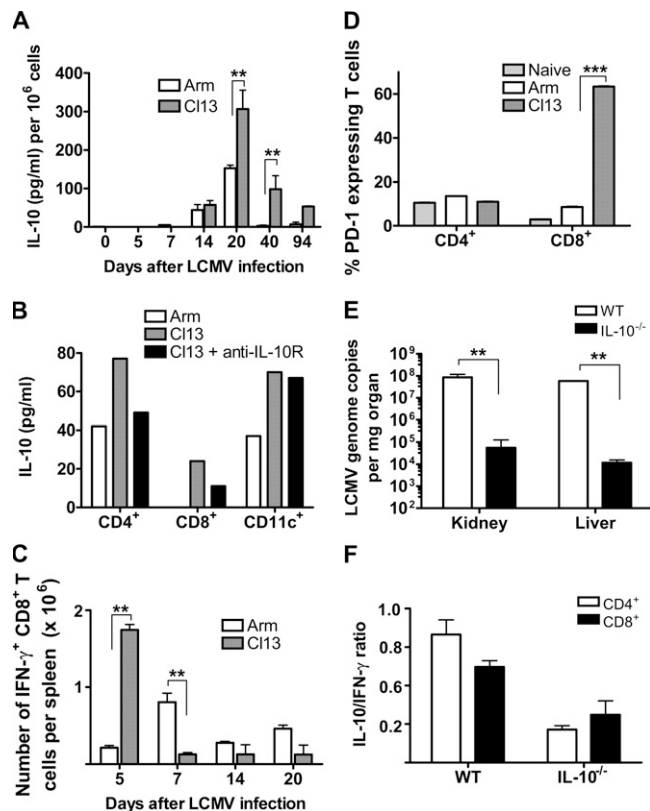### Persistent infection with LCMV clone 13 is associated with increased IL-10 production

Previous studies reporting IL-10 production during chronic viral infections prompted us to examine the secretion of IL-10 during chronic and acute LCMV infections (1, 12–19). Splenocytes from mice infected with LCMV clone 13 or LCMV Armstrong were isolated at various time points after infection and cultured for 48 h in the absence of exogenous antigen (to allow for direct ex vivo presentation of viral antigens by splenic APCs). At the end of this culture period, we measured the concentration of IL-10 in the supernatants by ELISA. IL-10 production by splenocytes from mice infected with LCMV (both clone 13 and Armstrong strains) peaked at day 20 after infection (Fig. 1 A). However, splenocytes from mice infected with LCMV Armstrong secreted significantly less IL-10. This difference was apparent regardless of the initial dose of virus, as increasing the inoculum of LCMV Armstrong from 10^5 PFU to 2×10^6 PFU resulted in comparable kinetics of IL-10 secretion (unpublished data). By day 40, although IL-10 production was undetectable in LCMV Armstrong–infected mice, mice infected with LCMV clone 13 still produced significant amounts of this cytokine (Fig. 1 A). After in vitro LCMV clone 13 infection, we observed that IL-10 was produced by different immune cell types, including CD4^{+} and CD8^{+} T cells and CD11c^{+} DCs, whereas LCMV Armstrong infection induced less IL-10 production by CD4^{+} T cells and CD11c^{+} DCs and none by CD8^{+} T cells (Fig. 1 B). Interestingly, when splenic cell cultures were treated with a neutralizing anti–IL-10R monoclonal antibody (which specifically targets the IL-10R α chain) at the time of LCMV clone 13 infection in vitro, the levels of IL-10 produced by CD4^{+} T cells were reduced to those found in LCMV Armstrong–infected mice (Fig. 1 B).

We then analyzed in vivo IFN-γ secretion by CD8^{+} T cells at different time points after LCMV Armstrong and LCMV clone 13 infection (Fig. 1 C). Interestingly, CD8^{+} T cells from LCMV clone 13–infected mice secreted IFN-γ only during the early phase of infection (day 5), at a time when no IL-10 was yet detected (Fig. 1 A). However, IFN-γ secretion was almost completely lost at later time points, and high levels of IL-10 were produced (Fig. 1, A and C). In contrast, IFN-γ production by CD8^{+} T cells from LCMV Armstrong–infected mice peaked later (day 7) and was sustained in the form of a memory response (Fig. 1 C) (27). Secretion of TNF-α followed a similar profile (unpublished data). Increasing the dose of LCMV Armstrong did not induce earlier cytokine responses (unpublished data). These results indicate that LCMV clone 13 induces a faster antiviral response, possibly linked to a higher binding affinity of the virus to its α-dystroglycan receptor (43).

It has recently been shown that high expression of PD-1 is a characteristic of exhausted CD8^{+} T cells in LCMV clone 13–infected mice and that treatment with anti–PD-1 antibodies leads to the proliferation of antiviral T cells and the enhancement of viral clearance (33–36). We therefore analyzed PD-1 expression on T cells. We found that a small percentage of CD4^{+} and CD8^{+} T cells expressed PD-1 in naive mice (Fig. 1 D). Upon LCMV infection, significantly higher levels of PD-1 were expressed on CD8^{+} T cells isolated from LCMV clone 13–infected mice compared with LCMV Armstrong–infected mice (Fig. 1 D). In addition, the mean fluorescence intensity of PD-1 was increased in T cells from LCMV clone 13–versus LCMV Armstrong–infected mice (unpublished data).

Based on these findings, we hypothesized that the immune suppression mediated by LCMV clone 13 infection was caused by a shift from antiviral IFN-γ production to the secretion of the immunosuppressive cytokine IL-10. To investigate whether IL-10 was directly involved in the suppression of the antiviral immune response, we infected IL-10–deficient (IL-10^{−/−}) mice with LCMV clone 13 and monitored viral clearance. 3 wk after LCMV clone 13 infection, we found
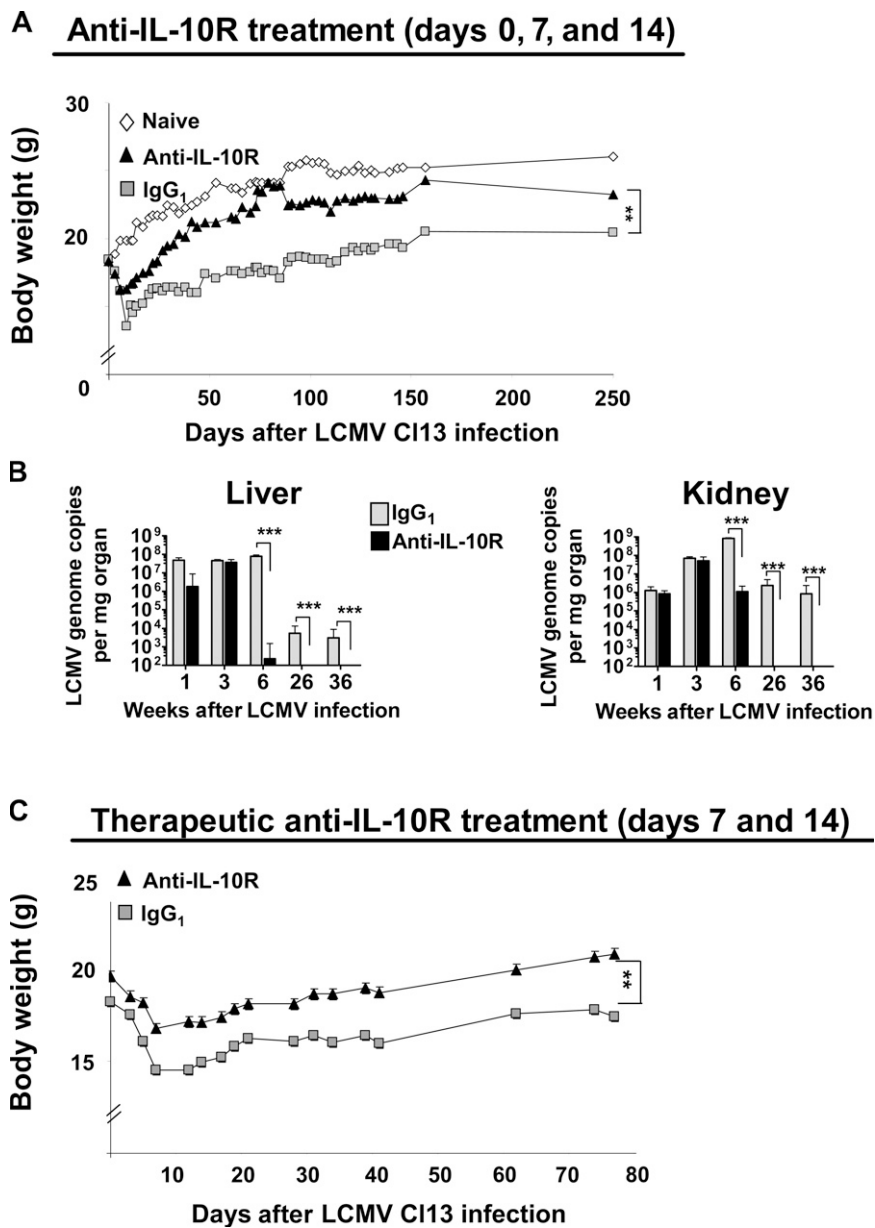
Figure 1. Time course of T cell cytokine production after infection with LCMV clone 13: the role of IL–10 in promoting viral persistence. (A) Spleen cells were isolated from BALB/c mice on days 0, 5, 7, 14, 20, 40, and 94 after infection with 10^5 PFU LCMV Armstrong or 2×10^6 PFU LCMV clone 13 and cultured for 48 h. The concentration of IL–10 present in the culture supernatants was measured by ELISA. Data are plotted as IL–10 (pg/ml) produced per 10^6 cells and are means of three mice per time point. The experiment is representative of three similar experiments. (B) To reveal the origin of IL–10–producing cell subsets, BALB/c splenocytes were isolated and infected in vitro for 48 h with LCMV Armstrong or LCMV clone 13 without or with anti–IL–10R antibody treatment (multiplicity of infection = 3). Next, $CD4^+$, $CD8^+$, and $CD11c^+$ cells were enriched using MACS beads, and the supernatant of the purified populations was analyzed for IL–10 production by ELISA. The graph indicates the levels of IL–10 (pg/ml) in the supernatant of $CD4^+$, $CD8^+$, and $CD11c^+$ cells. Data are representative of one experiment with five mice per group. (C) Sensitive direct in vivo intracellular cytokine assay was performed to detect in vivo cytokine expression in LCMV-specific T cells, as described by Liu et al. (reference 61). In brief, mice were injected i.v. with 0.5 mg BFA on days 5 and 7 after infection with 10^5 PFU LCMV Armstrong or 2×10^6 PFU LCMV clone 13. Spleens were harvested 6 h after BFA injection, and direct in vivo intracellular cytokine detection was performed after staining with fluorescent antibodies to CD4, CD8, IFN-γ, and TNF-α. Mean values per spleen of three to five individual mice are shown. The experiment is representative of two similar experiments. (D) PD-1 expression was detected on $CD4^+$ and $CD8^+$ T cells from naive or day 7 LCMV Armstrong– or LCMV clone 13–infected mice by labeling splenocytes with fluorescent antibodies to CD4, CD8, and PD-1. Percentages of PD-1–expressing T cells are shown. Data show one representative mouse per group (three mice total per group). (E) IL-10$^{-/-}$ and wild-type mice were infected with 2×10^6 PFU LCMV clone 13, and viral titers were detected in kidney and liver from three mice per group by RT-PCR 3 wk after

that viral titers were significantly lower in liver and kidney from IL-10$^{-/-}$ mice compared with wild-type control mice when measured by a highly sensitive RT-PCR method (Fig. 1 E). Resolution of LCMV clone 13 infection in IL-10$^{-/-}$ mice was associated with a lower systemic IL-10 to IFN-γ ratio, as one would expect (Fig. 1 F). Sustenance of antiviral immune responses to clone 13 through genetic elimination of IL-10 has been described in detail in another study by Brooks et al. (44).

Anti–IL–10R antibody therapy decreases viral titers and leads to disease amelioration

IL–10 can inhibit immune responses by skewing the development of helper T cells and suppressing their function (45, 46). Based on our initial findings that cells from LCMV clone 13–infected mice secreted IL-10 and that mice deficient in IL-10 cleared this strain of LCMV more efficiently, we investigated whether blocking the IL-10–IL-10R signaling pathway could resolve LCMV clone 13–induced immune suppression and reestablish an antiviral Tc1/Th1 response. We therefore infected BALB/c mice with LCMV clone 13 and injected age-matched groups with either a neutralizing anti–IL-10R monoclonal antibody or an IgG$_1$ isotype control antibody on days 0, 7, and 14, or with a therapeutic regimen on days 7 and 14 after infection. Disease severity was monitored by assessing bodyweight, spleen cell numbers, and viral titer over time. LCMV clone 13–infected mice treated with isotype control antibody lost body mass and weighed 30–40% less than age-matched naive mice (Fig. 2, A and C). These mice also exhibited a nonshiny, scruffy coat (unpublished data). In comparison, LCMV clone 13–infected mice treated with anti–IL-10R antibody lost weight less rapidly (Fig. 2 A) and exhibited a healthy shiny coat (not depicted). In addition, we monitored viral loads in lymphoid and nonlymphoid organs isolated from persistently infected mice treated with anti–IL-10R or IgG$_1$. Viral titers were measured by conventional plaque assay (not depicted) and by a more recently developed, highly sensitive RT-PCR method (Fig. 2 B). At 6 and 26 wk after infection, numbers of LCMV genomic copies were low or nondetectable when measured by the sensitive RT-PCR method in organs from anti–IL-10R–treated mice; 36 wk after infection, viral titers remained undetectable in liver and kidney (Fig. 2 B). In contrast, viral genome copies were still detectable in these organs when mice were treated with IgG$_1$ isotype antibody, indicating that resolution of chronic infection resulted from anti–IL-10R treatment rather than

infection. Data are shown as mean LCMV genome copies per mg organ $\pm$ SEM. (F) Cytokine expression was monitored in wild-type and IL-10$^{-/-}$ mice 7 d after LCMV clone 13 infection by intracellular cytokine staining. Splenocytes were stimulated with BFA and GP$_{33-41}$ or GP$_{61-80}$ peptide for 6 h. Intracellular cytokine detection was performed by staining with fluorescent antibodies to CD4, CD8, IFN-γ, and TNF-α. The IL-10/IFN-γ ratio of $CD4^+$ and $CD8^+$ T cells is shown as mean values of three individual mice per group. Statistical analysis was performed using the Student's t test. *, $P < 0.01$; **, $P < 0.001$; and ***, $P < 0.0001$.

A Anti-IL-10R treatment (days 0, 7, and 14)

B

C Therapeutic anti-IL-10R treatment (days 7 and 14)

Figure 2. Clearance of virus in LCMV clone 13–infected mice treated with anti–IL-10R antibody. 6-wk-old BALB/c mice were infected with 2×10^6 PFU LCMV clone 13 and treated i.p. with 250 μg of a neutralizing anti–IL-10R antibody or an IgG_1 isotype control antibody on days 0, 7, and 14 (A and B) or days 7 and 14 after infection (C). (A) Disease severity was evaluated by measuring the body weight of naive mice and LCMV clone 13–infected mice injected with anti–IL-10R antibody or IgG_1 isotype control antibody. Mice were monitored daily and weighed every third day. Data show mean body weight (in grams) ± SEM per group ($n = 5$) over time and are representative of five experiments (25 mice total per group). (B) Quantitative real time PCR for LCMV genome copies was performed on the cDNA obtained by reverse transcription in quick-frozen organs from LCMV clone 13–infected mice treated with IgG_1 isotype control or anti–IL-10R antibody. Liver (left) and kidney (right) were harvested 1, 3, 6, 26, and 36 wk after infection, and viral titers were measured by quantitative RT-PCR. Quantitative analysis was performed using the GraphPad Prism linear regression method. Histogram bars represent means values ± SD for four to six mice per group. The experiment is representative of five similar experiments. (C) Disease severity was evaluated by measuring body weight as described in A in mice treated therapeutically with anti–IL-10R antibody or IgG_1 isotype control antibody on days 7 and 14 after LCMV clone 13 infection. Data show mean body weight (in grams) ± SEM per group ($n = 5$) over time and are representative of two experiments (25 mice total per group). Statistical analysis was performed using the Student's t test. **, $P < 0.001$; and ***, $P < 0.0001$.

progressive viral elimination over time. Viral titers in organs from control IgG_1-treated mice remained high, and virus predominated in the kidney, characterizing the chronic infec-

tion (Fig. 2 B). Furthermore, extremely low viral titers were detected by LCMV plaque assay in kidney, liver, and lung 6 wk after LCMV clone 13 infection in anti–IL-10R–treated

mice, and no virus was detected 26 wk after infection (unpublished data).

Importantly, we also administered anti–IL-10R antibody in a therapeutic setting at days 7 and 14 after infection during the onset of lymphopenia and weight loss (by day 7 after infection, the total number of splenocytes was reduced by 41% in LCMV clone 13–infected mice compared with naive mice; unpublished data). Anti–IL-10R treatment was therapeutically effective during established infection as treated mice lost weight less rapidly (Fig. 2 C), did not exhibit any overt signs of disease, and showed a substantial reduction in viral titers in the liver, lung, and kidney 11 wk after treatment (not depicted). Additionally, a two to three log reduction in viral titer was observed when anti–IL-10R was given on days 5 and 12 after LCMV clone 13 infection, as well as on days 10 and 17 after infection (unpublished data).

Interestingly, there was no difference in anti-LCMV–specific antibody production after anti–IL-10R treatment (unpublished data), indicating that viral clearance was the result of an enhancement of the antiviral T cell responses. These results demonstrate that blocking IL-10 signaling results in clearance of an otherwise protracted LCMV clone 13 infection. Notably, anti–IL-10R treatment was effective even when given therapeutically during established infection.

Anti–IL-10R treatment of persistently infected mice restores antiviral CD8+ T cell responses

As reported previously (31, 47), we found that chronic infection was associated with deletion of virus-specific CD8+ T cells, leading to a drastic decrease in the number of spleen cells (unpublished data). We discovered that this state of lymphopenia was reversed after anti–IL-10R therapy both when treatment was initiated at day 0 or therapeutically at day 7 after infection (Fig. 3 A). In addition, endogenous IL-10 production by splenocytes isolated 3 wk after LCMV clone 13 infection was significantly reduced in anti–IL-10R–treated mice, indicating that early blockade of this cytokine prevented the long-term immunosuppressive effects mediated by LCMV clone 13 infection (Fig. 3 B).

We therefore assessed the effect of anti–IL-10R treatment on the LCMV-specific T cell response in detail. Splenocytes from anti–IL-10R– and control IgG₁–treated BALB/c mice were isolated at various time points after LCMV clone 13 infection and stimulated with the MHC class I–restricted immunodominant LCMV peptide $NP_{118-126}$. The number of IFN-γ–secreting CD8+ cells was measured by intracellular cytokine staining. Anti–IL-10R–treated mice had significantly higher numbers of IFN-γ–secreting CD8+ T cells compared with IgG₁-treated mice, particularly at later time points (Fig. 3 C). Importantly, therapeutic treatment with anti–IL-10R on days 7 and 14 after LCMV clone 13 infection caused a similar enhancement of the LCMV-specific memory T cell response (Fig. 3 C). Thus, anti–IL-10R treatment resulted in reemergence of a potent antiviral IFN-γ+ CD8+ T cell response, indicating that events occurring early during T cell responses can profoundly affect the quality of

T cell memory. It will be difficult to determine whether the enhancement of viral-specific CD8+ T cell responses was the cause or consequence of reduced viral loads; however, we believe that both alternatives are possible.

Finally, we investigated the effect of anti–IL-10R treatment on the PD-1 inhibitory pathway (33–36). To determine whether suppression of the PD-1 pathway could be involved in the enhancement of viral clearance after therapeutic anti–IL-10R treatment, we monitored expression of PD-1 by T cells in anti–IL-10R– and IgG₁-treated mice 90 d after LCMV clone 13 infection. Low levels of PD-1 expression were detected on T cells from naive mice (Fig. 3 D, top). In comparison, T cells from LCMV clone 13–infected mice treated with IgG₁ isotype antibody exhibited as much as a 25-fold induction of PD-1 expression compared with naive mice (Fig. 3 D, bottom). Importantly, a threefold reduction of PD-1 expression was observed on T cells from anti–IL-10R–treated mice compared with IgG₁-treated mice (Fig. 3 D, middle). These results indicate that anti–IL-10R treatment decreased PD-1 expression on T cells, which could potentially contribute to abrogation of T cell exhaustion because treatment with anti–PD-1 antibodies in chronically infected mice has been shown to down-regulate PD-1 and circumvent virally induced CD8+ T cell exhaustion (33–36).

Anti–IL-10R treatment reverses lymphopenia in LCMV clone 13–infected mice

To further investigate the effect of anti–IL-10R treatment on the LCMV-specific immune response, we examined absolute numbers of different splenic cell subsets over time in mice infected with LCMV clone 13 and treated with anti–IL-10R or control IgG₁ antibody. We discovered that even though LCMV clone 13 infection caused a reduction in the numbers of cells present in the spleen at day 21 after infection regardless of treatment, by day 150 after infection the numbers of CD4+, CD8+, B220+, and CD11c+ cells in anti–IL-10R–treated mice were similar to those in naive mice, whereas in IgG₁-treated mice these cells remained scarce (Fig. 4 A). Notably, the numbers of CD11b+ cells in the spleen at day 150 after infection were comparable between groups, suggesting that the decrease in viral titers after anti–IL-10R treatment was not solely caused by enhanced clearance of virally infected macrophages.

CD8α+ DCs are eliminated after LCMV clone 13 but not LCMV Armstrong infection

We hypothesized that the loss of antiviral T cells after LCMV clone 13 infection would be mediated by APCs. DCs are the most potent APCs and have been shown to play a crucial role in the priming of LCMV-specific cytotoxic T cells (48). We therefore examined absolute numbers of different DC subsets (CD11c+CD8α– and CD11c+CD8α+) and their ratio after infection with LCMV Armstrong or LCMV clone 13. Over the course of infection, the number of CD8α– and CD8α+ DCs increased in LCMV Armstrong–infected mice but returned to that found in naive mice within 2 wk after infection
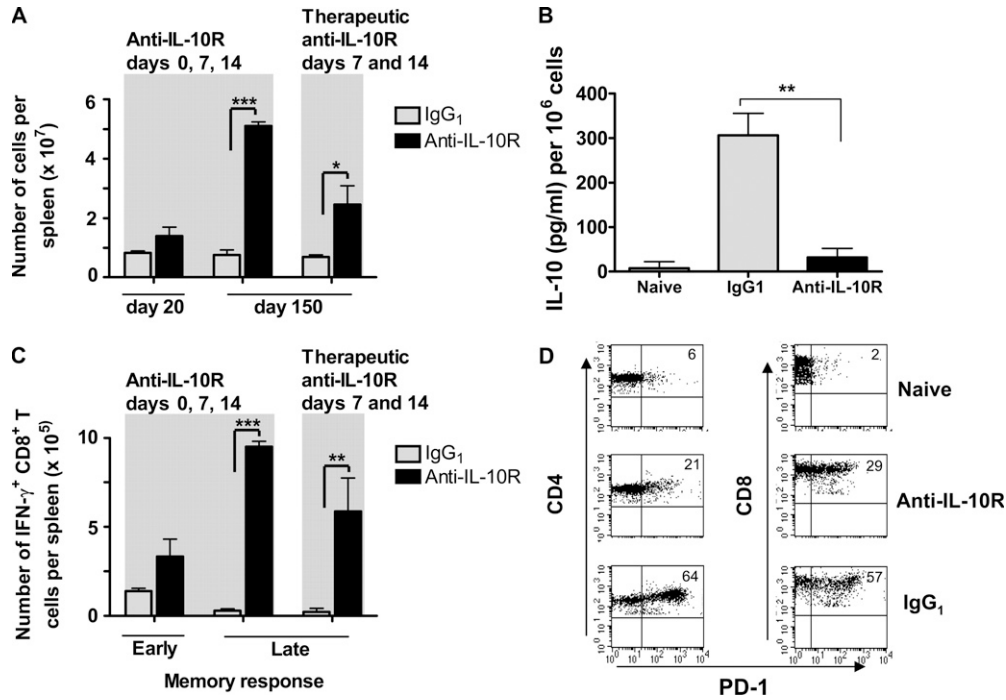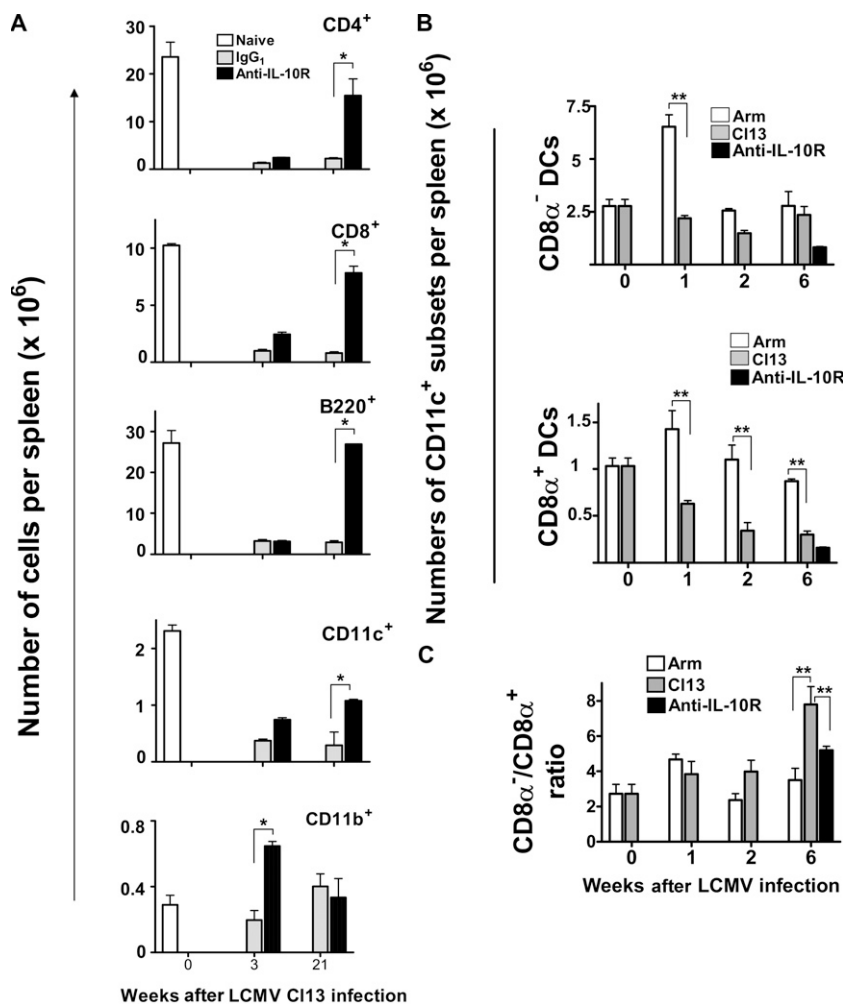
Figure 3. Anti–IL-10R antibody treatment in LCMV clone 13–infected mice increases total cell numbers, decreases IL-10 production, induces a functional antiviral memory T cell pool, and reduces the percentage of PD-1–expressing T cells. (A) 6-wk-old BALB/c mice were infected with 2×10^6 PFU LCMV clone 13 and treated with an IgG$_1$ isotype control antibody or i.p. with 250 μg of a neutralizing anti–IL-10R antibody on days 0, 7, and 14 (left) or with a therapeutic regimen on days 7 and 14 after LCMV clone 13 infection (right). On days 20 and 150 after LCMV infection, spleen cells were isolated and counted. Histogram bars represent mean values ± SD for three mice per group. The experiment is representative of three similar experiments. (B) Splenocytes from naive mice, LCMV clone 13–infected mice treated with IgG$_1$, or anti–IL-10R antibody on days 0, 7, and 14 were isolated 3 wk after infection and cultured for 48 h. The amount of IL-10 present in the culture supernatant was measured by ELISA. Data are plotted as IL-10 (pg/ml) produced per 10^6 cells and are means of three mice per time point. Results are representative of three identical experiments. (C) Splenocytes from LCMV clone 13–infected BALB/c mice treated with IgG$_1$ or anti–IL-10R antibody on days 0, 7, and 14 (left) or day 7 and 14 (right) were isolated at day 20 (early memory) and 150 (late memory) after infection. Cells were stimulated in the presence of NP$_{118-126}$ peptide and BFA for 5 h. Intracellular cytokine staining was performed using fluorescent antibodies to CD8 and IFN-γ. The numbers of IFN-γ$^+$CD8$^+$ T cells per spleen are shown. Histogram bars represent mean values ± SD for three mice per group. The experiment is representative of three similar experiments. (D) BALB/c mice were treated with anti–IL-10R antibody or IgG$_1$ isotype control antibody on days 7 and 14 after LCMV clone 13 infection. 90 d after infection, percentages of PD-1–expressing splenic CD4$^+$ and CD8$^+$ T cells were analyzed by gating on CD4$^+$ (left) and CD8$^+$ T cells (right) and staining for PD-1. Numbers in dot plots represent percentages of CD4$^+$ and CD8$^+$ T cells expressing PD-1. Data show one representative mouse per group (four mice total per group). Statistical analysis was performed using the Student's t test. *, $P < 0.01$; **, $P < 0.001$; and ***, $P < 0.0001$.

(Fig. 4 B). In contrast, although the number of CD8α$^-$ DCs from LCMV clone 13–infected mice 6 wk after infection was also comparable to that of naive mice, CD8α$^+$ DCs gradually disappeared over time (Fig. 4 B). It has been previously shown that >50% of CD11c$^+$ DCs carry viral particles at this time point in clone 13–infected mice (49), making these cells an excellent target for destruction and elimination by the immune system. In contrast, very few CD11c$^+$ cells are infected at the same time point after LCMV Armstrong infection (49). Importantly, the numbers of CD8α$^+$ DCs were significantly lower in LCMV clone 13–infected mice 6 wk after infection compared with mice infected with LCMV Armstrong (Fig. 4 B). Because the CD8α$^+$ DC subset declined in LCMV clone 13–infected mice and the CD8α$^-$ DC subset remained at a stable level, the CD8α$^-$ to CD8α$^+$ DC ratio was skewed toward CD8α$^-$ DCs 6 wk after infection (Fig. 4 C). To investigate whether this phenomenon was affected by therapeutic anti–IL-10R treatment, absolute numbers of CD8α$^-$ and CD8α$^+$ DCs were monitored 6 wk after LCMV clone 13 infection in mice treated with anti–IL-10R on days 7 and 14 after infection. Anti–IL-10R treatment decreased CD8α$^-$ DC numbers more than twofold, as well as CD8α$^+$ DC numbers to a lesser extent (Fig. 4 B). Hence, the resulting CD8α$^-$ to CD8α$^+$ DC ratio after anti–IL-10R treatment resembled the ratio in LCMV Armstrong–infected mice 6 wk after infection (Fig. 4 C). In summary, these findings show that anti–IL-10R treatment in LCMV clone 13–infected mice resulted in a skewing of the CD8α$^-$ to CD8α$^+$ DC ratio to levels seen in mice infected with the nonpersistent LCMV Armstrong strain.

Figure 4. Anti–IL-10R treatment restores cell numbers in LCMV clone 13–infected mice and resets the CD8α⁻ versus CD8α⁺ DC ratio to levels observed in LCMV Armstrong–infected mice. (A) The effect of 250 μg anti–IL-10R antibody (i.p.) or IgG₁ isotype control antibody treatment on different splenic cell subsets was monitored quantitatively. Spleens of mice infected 3 or 21 wk earlier with LCMV clone 13 were harvested, and cell suspensions were stained with fluorescent antibodies to CD4, CD8, B220, CD11c, and CD11b. Age-matched naive mice were included as controls. Numbers of cells were quantified by relating the percentage to total numbers of spleen cells. Mean values for three to five individual mice are shown. Results are representative of three similar experiments. (B and C) The total numbers of CD11c⁺CD8α⁻ (B, top) or CD11c⁺CD8α⁺ splenic DC subsets (B, bottom) and the CD8α⁻ to CD8α⁺ DC ratios (C) were

determined 0, 1, 2, and 6 wk after LCMV Armstrong or LCMV clone 13 infection. In addition, absolute splenic DC subsets (B) and the CD8α⁻ to CD8α⁺ DC ratio (C) were calculated from mice therapeutically treated with anti–IL10R on days 7 and 14 after LCMV clone 13 infection; the latter was examined at 6 wk after infection only. Cell suspensions were prepared by digestion with collagenase D. Cells were then stained with fluorescent antibodies to CD11c, CD3, and CD8α. The percentage of CD8α⁻ and CD8α⁺ within the CD11c⁺CD3⁻ subset was determined by flow cytometry, and total numbers per spleen were quantified by relating the percentage of these cells to total numbers of CD11c⁺CD3⁻ spleen cells. Histogram bars represent mean values ± SD for three mice per group. The experiment is representative of three similar experiments. Statistical analysis was performed using the Student's t test. *, P < 0.01; and **, P < 0.001.

CD8α⁻ DCs preferentially prime IL-10 production during the development of chronic infection

Previous reports suggest that different DC subsets vary in their ability to prime effector T cells (39, 50, 51). In particular, evidence suggests that different DC subsets can induce T cells to produce different cytokines depending on the cytokine milieu in which they encounter antigen (40, 41, 46). We therefore investigated whether T cell priming by different DC subsets modulated the nature of the antiviral T cell

response. CD11c⁺CD3⁻ splenic DCs were isolated from mice infected 7 d earlier with LCMV Armstrong or LCMV clone 13. In addition, one group of mice was treated with anti–IL-10R antibody at the time of infection. CD11c⁺CD3⁻ DCs from all groups were sorted into CD8α⁻ and CD8α⁺ DC subsets on day 7 after infection (Fig. 5). This early time point was chosen to allow for capture and processing of viral antigens by DCs directly in vivo during the early phase of LCMV Armstrong and LCMV clone 13 infection, which is

associated with viral dissemination and replication. At this time, viral antigen could be detected by RT-PCR (unpublished data). Because we had previously observed that CD4^{+} T cells from LCMV clone 13–infected mice produced elevated levels of IL-10, the isolated DCs were cultured for 5 d with naive GP$_{61-80}$-specific CD4^{+} responder T cells isolated from TCR transgenic SMARTA mice (52). No exogenous antigen was added to the cultures to ensure that only viral antigen processed in vivo was presented by the DCs. The ability of the different DC subsets to stimulate LCMV-specific CD4^{+} T cells was determined by measuring the concentration of cytokines in the supernatants by ELISA at the end of the culture period. To rule out any contamination caused by cytokine release by APCs, DCs were irradiated, and levels of both IL-10 and IFN-γ were measured in the supernatants of DC cultures devoid of T cells. These background levels were <1 pg/ml (unpublished data).

IL-10 production by antiviral CD4^{+} T cells was induced exclusively by DCs isolated from LCMV clone 13–infected mice and was preferentially mediated by the CD8α^{−} DC subset (Fig. 5 A), an observation that was confirmed when the different DC subsets were loaded with LCMV GP$_{61-80}$ peptide (not depicted). Importantly, this corresponded to the time point at which CD8α[+] DC numbers in LCMV clone 13–infected mice started to decline (Fig. 4 B). These results suggest that when CD8α[+] DCs are infected and killed, the remaining CD8α[−] DCs that are left to prime T cells induce IL-10 production instead of a potent antiviral response. In contrast, CD8α^{−} or CD8α^{+} DCs isolated from mice infected with LCMV Armstrong induced little to no IL-10 production by LCMV-specific CD4^{+} T cells (Fig. 5 A), indicating that differences between the two LCMV infections could merely reside in the type of cytokine responses induced. In vivo anti–IL-10R treatment completely abrogated the capacity of CD8α^{−} DCs to induce IL-10 secretion in CD4^{+} T cells (Fig. 5 A), indicating that signaling through the IL-10R was crucial for CD8α^{−} DCs to induce IL-10.

Additionally, both CD8α^{−} and CD8α^{+} DCs from LCMV clone 13– and LCMV Armstrong–infected mice were able to stimulate IFN-γ production by CD4^{+} T cells, whereas CD8α^{+} DCs induced higher amounts of IFN-γ than CD8α^{−} DCs. Anti–IL-10R treatment did not have an effect on IFN-γ production induced by the different DC subsets (Fig. 5 B).

Importantly, although the amount of IL-10 induced by CD8α[−] and CD8α[+] DC subsets was dependent on the LCMV strain used (Fig. 5 A), the amount of IFN-γ was similar for both LCMV strains (Fig. 5 B). Therefore, the IL-10 to IFN-γ ratio was always significantly higher when DCs from LCMV clone 13–infected mice were used as APCs (Fig. 5 C).

Collectively, these data show that anti–IL-10R treatment abolished CD8α[−] DC-mediated IL-10 production in responder T cells early after infection and decreased absolute CD8α[−] DC numbers over time, thereby inducing a shift toward IFN-γ[+] and Tc1/Th1 responses, enabling viral
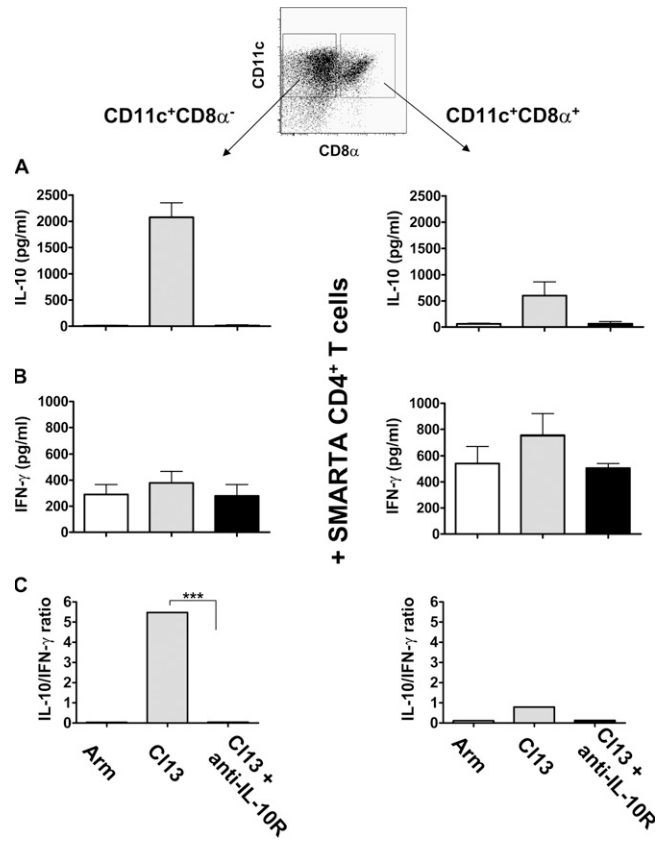
Figure 5. **Anti–IL-10R treatment abolishes IL-10 production by CD8α[−] and CD8α[+] DC subsets, restoring a Tc1/Th1-favorable environment.** Spleens were isolated and pooled from mice 7 d after infection with LCMV Armstrong or LCMV clone 13 or from LCMV clone 13–infected mice treated with anti–IL-10R antibody at the time of infection (8–10 mice per group). Splenocytes were depleted of CD3^{+} cells and enriched based on expression of CD11c using MACS microbeads. Next, the purified CD11c^{+} population was labeled with fluorescent antibodies to CD11c and CD8α and sorted into CD11c^{+}CD8α^{−} (left) or CD11c^{+}CD8α^{+} DCs (right) by flow cytometry. The sorted DCs were irradiated (2,900 rad), and 1.5×10^5 DCs from each subset were cultured in U-bottom 96-well plates in the presence of 6×10^5 GP$_{61-80}$-specific CD4^{+} T cells isolated from naive TCR transgenic SMARTA mice (reference 52). After 5 d, the concentration of IL-10 (A) and IFN-γ (B) present in the culture supernatants was measured by ELISA (pg/ml). No detectable IL-10 or IFN-γ was secreted by irradiated DCs alone (not depicted). Data was obtained from two independent experiments. Histogram bars represent mean values from one representative experiment ± SD from triplicate wells. (C) The results are depicted as the IL-10 to IFN-γ ratio to reflect the overall trend toward IL-10 production by the stimulated CD4^{+} T cells. Statistical analysis was performed using the Student's t test. ***, P < 0.0001.

clearance. Our observations that anti–IL-10R antibody led to resolution of protracted infection, enhanced antiviral T cell responses, and abrogated the ability of CD8α^{−} DCs to induce IL-10 in CD4^{+} T cells, in conjunction with observed lower viral titers in mice deficient in IL-10, underscores the important role IL-10 plays in maintaining a chronic viral infection.

DISCUSSION

This study is the first to report that inhibiting IL-10 signaling in vivo leads to enhancement of viral clearance in a mouse model of persistent viral infection. Our data demonstrate that upon challenge with LCMV clone 13, the strong antiviral response elicited early after infection rapidly subsides and is followed by a state of chronic infection associated with generalized lymphopenia. In this paper, we show that chronic infection and deterioration in health is associated with systemic increase in the production of IL-10. Although the implication for the role of IL-10 in the maintenance of chronic viral infections has hitherto been unclear, our results show that lymphopenia is reversed, bodyweight recovers, and viral load is significantly reduced upon blockade of IL-10–IL-10R signaling ($P < 0.0001$). Furthermore, we show that anti–IL-10R treatment results in a reduction of CD8α^- DC numbers and a subsequent abolishment of IL-10 production, thereby favoring a Tc1/Th1 cell–like environment inducing LCMV-specific IFN-γ^+ T cell responses. Indeed, after LCMV clone 13 infection, CD8α^+ DC numbers substantially were found to decrease because of viral infection and clearance, and we now show that CD8α^- DCs will preferentially induce IL-10 production by T cells. Thus, it is possible that the generalized state of lymphopenia of LCMV clone 13–infected mice is mediated by APCs inducing IL-10–producing T cells, which results in a negative feedback loop. Our results suggest that distinct DC subsets may differentially regulate the cytokine balance of the immune response in vivo. The precise mechanism by which these DC subsets mediate their effects might be related to levels of IL-10 present in the microenvironment. We show that CD8α^- DCs induce IL-10 production more efficiently than their CD8α^+ counterparts. The ability to potentiate IL-10 secretion is drastically reduced upon blockade of signaling through the IL-10R. We believe that anti–IL-10R treatment modulates CD8α^- DCs early upon infection and, as a result, dictates the nature of the cytokine response induced early during antiviral immunity.

The mechanisms by which IL-10 enables LCMV clone 13 to persist are unknown. Several variables associated with T cell priming have been shown to be important and may program qualitative differences into the effector and memory populations (53). IL-10 could either down-regulate proinflammatory responses in a general manner or, more specifically, inhibit the induction or expansion of antiviral CD8$^+$ effector T cells. Importantly, we report for the first time that anti–IL-10R antibody treatment reduces PD-1 expression on CD8$^+$ T cells, which has previously been shown to contribute to virally induced CD8$^+$ T cell exhaustion (33–36). Interestingly, stimulation through TLR2, which has been shown to bind to LCMV, leads to the production of IL-10 and inhibits IFN-inducible protein 10 and IL-12 secretion by APCs. Thus, stronger binding of LCMV clone 13 to TLR2, as opposed to weaker TLR2 binding by LCMV Armstrong (54), could not only induce preferential production of IL-10 by DCs but also inhibit the secretion of cytokines that promote DC differentiation, maturation, and proliferation rather

than survival (49). In addition, it is possible that the DCs that remain after LCMV clone 13 infection express higher levels of TLR2, thus perpetuating the cycle.

Subclasses of DCs have been shown to have the potential to differentially skew T cell cytokine production toward Th1 or Th2 cell profiles (40, 41, 55). Notably, it has been suggested that CD8α^- DCs induce Th2 cell profiles, whereas CD8α^+ DCs preferentially stimulate IFN-γ production and, therefore, induce Th1 cell profiles (39, 51). We now show that this may be true in the LCMV system, as we have analyzed the ability of CD8α^- and CD8α^+ DCs to polarize LCMV-reactive CD4$^+$ T cells ex vivo. It appears that priming of cytotoxic T lymphocytes by DCs is achieved in a similar fashion in LCMV clone 13– and LCMV Armstrong–infected mice, but that stronger binding of LCMV clone 13 to its receptor on APCs, particularly CD8α^+ DCs, leads to more efficient processing and presentation of viral antigen. Our finding that LCMV clone 13 infection leads to early induction of IFN-γ–secreting LCMV-specific CD8$^+$ T cells strengthens this hypothesis. The strong cytotoxic function of such activated Tc1 or Th1 cells upon infection with LCMV clone 13 may result in killing of the APC subset responsible for their induction; i.e., DCs belonging to the CD8α^+ subset. This hypothesis correlates with our finding that the number of CD8α^+ DCs is reduced as early as day 7 after infection with LCMV clone 13 but not LCMV Armstrong.

Our results suggest that as the number of CD8α^+ DCs decreases after chronic LCMV clone 13 infection, the CD8α^- DC subset—which is more likely to prime T cells to produce IL-10 than Tc1/Th1 cytokines—will by default become the modulator of the T cell response. LCMV-specific CD4$^+$ T cells activated in this context may provide inappropriate or insufficient antiviral help to other cell types, particularly CD8$^+$ T cells, thus leading to persistent infection. Additionally, it is possible that the CD8α^- DCs, which appear ill-equipped to propagate antiviral effectors, will continue to support IL-10 production. The resulting high concentration of IL-10 in the milieu may thus lead to further modulation of DC function. In fact, IL-10 may directly decrease the viability of CD8α^+ DCs, as has been previously suggested (40, 56). As a result, only disruption of IL-10 signaling will have the ability to break the vicious circle and enable the recovery of appropriate antiviral immunity by the infected host.

Mechanistically, our findings show that anti–IL-10R antibody treatment lowers the endogenous levels of IL-10, restores the ability to mount an antiviral CD8$^+$ T cell response, and results in enhanced viral clearance, which all highlight the important role IL-10 plays in the maintenance of chronic infection. Upon treatment with anti–IL-10R, we observed a profound decrease in CD8α^- and, to a lesser degree, in CD8α^+ DC numbers, as well as a complete inability of CD8α^- DCs to induce IL-10 production by CD4$^+$ responder T cells, thereby favoring a systemic cytokine milieu that would better support IFN-γ^+ and Tc1/Th1 cell responses.

Importantly, the inability of CD8α^- DCs to induce IL-10 production by CD4$^+$ T cells after anti–IL-10R treatment

underscores that IL-10 and signaling through the IL-10R is indeed involved in shaping the cytokine milieu with a potential impact on immune responses. Our results imply that IL-10R blockade is of great interest for the therapeutic treatment of chronic viral infections in humans.

MATERIALS AND METHODS

Mice, virus, and antibody treatment. 6-wk-old BALB/c, C57BL/6 (B6), and IL-10$^{-/-}$ (B6 background) mice were purchased from The Jackson Laboratory. LCMV-GP$_{61-80}$–specific CD4$^+$ TCR transgenic SMARTA mice (52) were obtained from S. Crotty (La Jolla Institute for Allergy and Immunology, La Jolla, CA) and housed under specific pathogen-free conditions at the La Jolla Institute for Allergy and Immunology. LCMV plaques were purified three times on Vero cells, and viral stocks were prepared by a single passage on BHK-1 cells. Age-matched mice were infected i.v. with a single dose of either 2×10^6 PFU LCMV clone 13, 2×10^6 LCMV Armstrong, or an i.p. dose of 10^5 PFU LCMV Armstrong. For IL-10 blocking experiments, mice were injected i.p. with 250 μg anti–mouse IL-10R (1B1.3a; Becton Dickinson) monoclonal antibody or isotype control antibody (rat IgG1; BD Biosciences). All animal experiments were approved by the La Jolla Institute for Allergy and Immunology Animal Care Committee.

LCMV plaque assay. Organs (kidney, liver, spleen, and lung) were snap-frozen, weighed, and homogenized. In brief, three different dilutions of homogenized organ were prepared, and triplicates were used. Dilutions were incubated at 37°C, 5% CO_2 for 1 h with Vero cell monolayers grown in 6-well plates (Costar). The plates were then overlaid with 1% agarose in minimal essential medium 199 (Invitrogen) containing 10% FCS (Hy-Clone) and incubated at 37°C, 5% CO_2 for 5 d. The wells were treated with 25% formaldehyde and stained with 0.1% crystal violet for 2 min. The agarose overlay was removed, infectious centers were counted, and the counts were averaged. Additionally, viral LCMV stock was used as a positive control.

RT-PCR. A detailed version of this assay will be published elsewhere (unpublished data). In brief, RNA was isolated from 50 μl of serum or 10 mg of tissue samples using RNAqueous (Ambion). All samples were frozen at −80°C until RNA extraction. RNA was eluted in a volume of 20 μl, and purified RNA was frozen at −80°C until further use. 10 μl RNA was used in a 20-μl cDNA reaction with SuperScript III reverse transcriptase (Invitrogen) and a gene-specific primer (GP-R, GCAACTGCTGTGTTCCCGAAAC). 5 μl cDNA was used as template for a 25-μl quantitative real-time PCR reaction on a GeneAmp 5700 (ABI), using primers GP-R and GP-F (CATTC-ACCTGGACTTTGTCAGACTC). A standard curve was generated using pSG5-GP plasmid (57), a gift from J.C. de la Torre (Scripps Research Institute, San Diego, CA). Data were analyzed using linear regression analysis software (Prism; GraphPad).

Quantification of cytokines. Cytokine quantification was performed by sandwich ELISA of supernatants. $2–5 \times 10^6$ splenocytes were incubated for 48 h in complete RPMI 1640 (Invitrogen) supplemented with 10% FCS (Sigma-Aldrich), 2 mM L-glutamine (Sigma-Aldrich), 50 μM 2-β-mercaptoethanol (Sigma-Aldrich), and 5 mM Hepes (Sigma-Aldrich) in 24-well plates (Invitrogen). For the detection of IL-10–secreting cell subsets from in vitro infected cultures, bulk splenocytes were infected in vitro with LCMV Armstrong or LCMV clone 13 (multiplicity of infection = 3) without or with 10μg/ml anti–IL-10R antibody and incubated at 37°C in complete RPMI 1640. 48 h after infection, splenocytes were sorted into CD4$^+$, CD8$^+$, and CD11c$^+$ populations by MACS, and equal numbers of each cell subset were incubated for 5 d at 37°C. Supernatant was removed at the time points indicated in the figures, and ELISA was performed in accordance with the manufacturer's recommendations and standardized with mouse recombinant cytokine (BD Biosciences). Plates were read at 405 nm (Spectra Max 250; Molecular Devices). The sensitivity of the IL-10 ELISA was 10 pg/ml. Data shown correspond to the concentration of IL-10 (pg/ml) per 10^6 cells.

Intracellular cytokine staining, cell surface staining, and flow cytometry. To detect cytokine-producing cell subsets, splenocytes from LCMV-infected BALB/c or B6 mice were stimulated with 1 μg/ml NP$_{118-126}$, GP$_{33-41}$, or GP$_{61-80}$ peptide, respectively, in complete RPMI 1640 containing Brefeldin A (BFA; Sigma-Aldrich) at 37°C. 6 h later, cells were resuspended in staining buffer containing 1% FCS and 0.2% NaN$_3$, labeled with anti-CD4 and anti-CD8, fixed in 1% paraformaldehyde, and permeabilized with 0.1% saponin buffer. Intracellular staining was performed with fluorescent antibodies to IFN-γ, TNF-α, or isotype controls. All antibodies were obtained from BD Biosciences. Additionally, PD-1 expression was detected on splenocytes by labeling with an anti–PE-conjugated PD-1 antibody (eBioscience). Events were acquired using a flow cytometer (FACSCalibur; Becton Dickinson) and analyzed using software (CellQuest; Becton Dickinson). $1–2 \times 10^4$ events were acquired, and live cells were gated based on forward/side scatter properties. When analyzing CD11c$^+$ subsets, CD3-expressing cells were gated out to avoid contamination by T cells expressing myeloid markers (58, 59), and expression of the indicated cell surface molecules was detected on CD11c$^+$ and CD8α$^{+/-}$ cells. The number of cells was calculated by relating the frequency of cells from each subset to the overall number of cells per spleen.

Sorting of CD11c$^+$CD8α$^-$ and CD11c$^+$CD8α$^+$ cells. Splenocytes from mice infected 7 d earlier with LCMV Armstrong or LCMV clone 13 with or without anti–IL-10R antibody treatment were incubated with HBSS medium containing 0.5 mg/ml collagenase D (Sigma-Aldrich) at 37°C, 5% CO_2 for 30 min. 0.01 M EDTA was added to disrupt T cell–DC complexes. Next, cells were depleted of CD3-expressing cells (Dynal CD3-beads; Dynal), incubated with CD11c microbeads (Miltenyi Biotec), and positively selected using MACS columns. The enriched CD11c$^+$ cells were labeled with APC-conjugated CD11c and PE-conjugated CD8α antibody (BD Biosciences) and sorted using a cell sorter (FACS Aria; Becton Dickinson) into CD8α$^-$ and CD8α$^+$ CD11c$^+$ subsets. 1.5×10^5 sorted CD11c$^+$ cells were placed in 96-well plates in complete RPMI 1640 medium and irradiated with 2,900 rad. Assessment of the polarization of antigen-specific CD4$^+$ T cells by DCs ex vivo was adapted from a previously described method (60). LCMV GP$_{61-80}$-specific CD4$^+$ T cells isolated from TCR transgenic SMARTA mice (52) were purified by negatively depleting CD8-, B220-, and CD11b-expressing cells with Dynal beads and, after enrichment of CD4$^+$ T cells, with CD4-MACS beads (purity > 98%). 6×10^5 CD4$^+$ cells were added to DCs in the presence or absence of 1 μg/ml GP$_{61-80}$ peptide. Supernatants were isolated 5 d later and analyzed for the presence of IL-10 and IFN-γ by ELISA, as reported earlier in this paper.

Statistical analysis. Statistical analyses were performed using the Student's *t* test: *, P < 0.01; **, P < 0.001; and ***, P < 0.0001.

REFERENCES

1. Moore, K.W., A. O'Garra, R. de Waal Malefyt, P. Vieira, and T.R. Mosmann. 1993. Interleukin-10. *Annu. Rev. Immunol.* 11:165–190.
2. Pestka, S., C.D. Krause, D. Sarkar, M.R. Walter, Y. Shi, and P.B. Fisher. 2004. Interleukin-10 and related cytokines and receptors. *Annu. Rev. Immunol.* 22:929–979.
3. Vicari, A.P., C. Chiodoni, C. Vaure, S. Ait-Yahia, C. Dercamp, F. Matsos, O. Reynard, C. Taverne, P. Merle, M.P. Colombo, et al. 2002. Reversal of tumor-induced dendritic cell paralysis by CpG immunostimulatory oligonucleotide and anti–interleukin-10 receptor antibody. *J. Exp. Med.* 196:541–549.
4. Vicari, A.P., and G. Trinchieri. 2004. Interleukin-10 in viral diseases and cancer: exiting the labyrinth? *Immunol. Rev.* 202:223–236.

2470

IL-10R BLOCKADE RESOLVES CHRONIC VIRAL INFECTION | Ejrnaes et al.

5. Orange, J.S., M.S. Fassett, L.A. Koopman, J.E. Boyson, and J.L. Strominger. 2002. Viral evasion of natural killer cells. *Nat. Immunol.* 3:1006–1012.

6. Benedict, C.A., P.S. Norris, and C.F. Ware. 2002. To kill or be killed: viral evasion of apoptosis. *Nat. Immunol.* 3:1013–1018.

7. Yewdell, J.W., and A.B. Hill. 2002. Viral interference with antigen presentation. *Nat. Immunol.* 3:1019–1025.

8. Rouse, B.T., and D.W. Horohov. 1986. Immunosuppression in viral infections. *Rev. Infect. Dis.* 8:850–873.

9. Pantaleo, G., and R.A. Koup. 2004. Correlates of immune protection in HIV-1 infection: what we know, what we don't know, what we should know. *Nat. Med.* 10:806–810.

10. Letvin, N.L., and B.D. Walker. 2003. Immunopathogenesis and immunotherapy in AIDS virus infections. *Nat. Med.* 9:861–866.

11. Rehermann, B., and M. Nascimbeni. 2005. Immunology of hepatitis B virus and hepatitis C virus infection. *Nat. Rev. Immunol.* 5:215–229.

12. Woitas, R.P., U. Petersen, D. Moshage, H.H. Brackmann, B. Matz, T. Sauerbruch, and U. Spengler. 2002. HCV-specific cytokine induction in monocytes of patients with different outcomes of hepatitis C. *World J. Gastroenterol.* 8:562–566.

13. Hofer, H., J.B. Neufeld, C. Oesterreicher, P. Grundtner, F. Wrba, A. Gangl, P. Ferenci, and C. Gasche. 2005. Bi-allelic presence of the interleukin-10 receptor 1 G330R allele is associated with cirrhosis in chronic HCV-1 infection. *Genes Immun.* 6:242–247.

14. Graziosi, C., G. Pantaleo, K.R. Gantt, J.P. Fortin, J.F. Demarest, O.J. Cohen, R.P. Sekaly, and A.S. Fauci. 1994. Lack of evidence for the dichotomy of TH1 and TH2 predominance in HIV-infected individuals. *Science.* 265:248–252.

15. Zanussi, S., C. Simonelli, M. D'Andrea, C. Caffau, M. Clerici, U. Tirelli, and P. DePaoli. 1996. CD8+ lymphocyte phenotype and cytokine production in long-term non-progressor and in progressor patients with HIV-1 infection. *Clin. Exp. Immunol.* 105:220–224.

16. Clerici, M., M.L. Fusi, S. Ruzzante, S. Piconi, M. Biasin, D. Arienti, D. Trabattoni, and M.L. Villa. 1997. Type 1 and type 2 cytokines in HIV infection–a possible role in apoptosis and disease progression. *Ann. Med.* 29:185–188.

17. Orandle, M.S., K.C. Williams, A.G. MacLean, S.V. Westmoreland, and A.A. Lackner. 2001. Macaques with rapid disease progression and simian immunodeficiency virus encephalitis have a unique cytokine profile in peripheral lymphoid tissues. *J. Virol.* 75:4448–4452.

18. Ostrowski, M.A., J.X. Gu, C. Kovacs, J. Freedman, M.A. Luscher, and K.S. MacDonald. 2001. Quantitative and qualitative assessment of human immunodeficiency virus type 1 (HIV-1)-specific CD4+ T cell immunity to gag in HIV-1–infected individuals with differential disease progression: reciprocal interferon-gamma and interleukin-10 responses. *J. Infect. Dis.* 184:1268–1278.

19. Swaminathan, S. 2003. Molecular biology of Epstein-Barr virus and Kaposi's sarcoma-associated herpesvirus. *Semin. Hematol.* 40:107–115.

20. Accapezzato, D., V. Francavilla, M. Paroli, M. Casciaro, L.V. Chircu, A. Cividini, S. Abrignani, M.U. Mondelli, and V. Barnaba. 2004. Hepatic expansion of a virus-specific regulatory CD8(+) T cell population in chronic hepatitis C virus infection. *J. Clin. Invest.* 113:963–972.

21. Oldstone, M.B. 2002. Biology and pathogenesis of lymphocytic choriomeningitis virus infection. *Curr. Top. Microbiol. Immunol.* 263:83–117.

22. Jamieson, B.D., L.D. Butler, and R. Ahmed. 1987. Effective clearance of a persistent viral infection requires cooperation between virus-specific Lyt2+ T cells and nonspecific bone marrow-derived cells. *J. Virol.* 61:3930–3937.

23. Zinkernagel, R.M., and P.C. Doherty. 1979. MHC-restricted cytotoxic T cells: studies on the biological role of polymorphic major transplantation antigens determining T-cell restriction-specificity, function, and responsiveness. *Adv. Immunol.* 27:51–177.

24. Oldstone, M.B., P. Blount, P.J. Southern, and P.W. Lampert. 1986. Cytoimmunotherapy for persistent virus infection reveals a unique clearance pattern from the central nervous system. *Nature.* 321:239–243.

25. Marker, O., and M. Volkert. 1973. Studies on cell-mediated immunity to lymphocytic choriomeningitis virus in mice. *J. Exp. Med.* 137:1511–1525.

26. Moskophidis, D., U. Assmann-Wischer, M.M. Simon, and F. Lehmann-Grube. 1987. The immune response of the mouse to lymphocytic choriomeningitis virus. V. High numbers of cytolytic T lymphocytes are generated in the spleen during acute infection. *Eur. J. Immunol.* 17:937–942.

27. Lau, L.L., B.D. Jamieson, T. Somasundaram, and R. Ahmed. 1994. Cytotoxic T-cell memory without antigen. *Nature.* 369:648–652.

28. Salvato, M., P. Borrow, E. Shimomaye, and M.B. Oldstone. 1991. Molecular basis of viral persistence: a single amino acid change in the glycoprotein of lymphocytic choriomeningitis virus is associated with suppression of the antiviral cytotoxic T-lymphocyte response and establishment of persistence. *J. Virol.* 65:1863–1869.

29. Ahmed, R., C.S. Hahn, T. Somasundaram, L. Villarete, M. Matloubian, and J.H. Strauss. 1991. Molecular basis of organ-specific selection of viral variants during chronic infection. *J. Virol.* 65:4242–4247.

30. Matloubian, M., T. Somasundaram, S.R. Kolhekar, R. Selvakumar, and R. Ahmed. 1990. Genetic basis of viral persistence: single amino acid change in the viral glycoprotein affects ability of lymphocytic choriomeningitis virus to persist in adult mice. *J. Exp. Med.* 172:1043–1048.

31. Moskophidis, D., F. Lechner, H. Pircher, and R.M. Zinkernagel. 1993. Virus persistence in acutely infected immunocompetent mice by exhaustion of antiviral cytotoxic effector T cells. *Nature.* 362:758–761.

32. Zajac, A.J., J.N. Blattman, K. Murali-Krishna, D.J. Sourdive, M. Suresh, J.D. Altman, and R. Ahmed. 1998. Viral immune evasion due to persistence of activated T cells without effector function. *J. Exp. Med.* 188:2205–2213.

33. Barber, D.L., E.J. Wherry, D. Masopust, B. Zhu, J.P. Allison, A.H. Sharpe, G.J. Freeman, and R. Ahmed. 2006. Restoring function in exhausted CD8 T cells during chronic viral infection. *Nature.* 439:682–687.

34. Ishida, Y., Y. Agata, K. Shibahara, and T. Honjo. 1992. Induced expression of PD-1, a novel member of the immunoglobulin gene superfamily, upon programmed cell death. *EMBO J.* 11:3887–3895.

35. Sharpe, A.H., and G.J. Freeman. 2002. The B7-CD28 superfamily. *Nat. Rev. Immunol.* 2:116–126.

36. Freeman, G.J., A.J. Long, Y. Iwai, K. Bourque, T. Chernova, H. Nishimura, L.J. Fitz, N. Malenkovich, T. Okazaki, M.C. Byrne, et al. 2000. Engagement of the PD-1 immunoinhibitory receptor by a novel B7 family member leads to negative regulation of lymphocyte activation. *J. Exp. Med.* 192:1027–1034.

37. Mosmann, T.R., and R.L. Coffman. 1989. TH1 and TH2 cells: different patterns of lymphokine secretion lead to different functional properties. *Annu. Rev. Immunol.* 7:145–173.

38. Kalinski, P., C.M. Hilkens, E.A. Wierenga, and M.L. Kapsenberg. 1999. T-cell priming by type-1 and type-2 polarized dendritic cells: the concept of a third signal. *Immunol. Today.* 20:561–567.

39. Maldonado-Lopez, R., T. De Smedt, P. Michel, J. Godfroid, B. Pajak, C. Heirman, K. Thielemans, O. Leo, J. Urbain, and M. Moser. 1999. CD8α+ and CD8α− subclasses of dendritic cells direct the development of distinct T helper cells in vivo. *J. Exp. Med.* 189:587–592.

40. Maldonado-Lopez, R., C. Maliszewski, J. Urbain, and M. Moser. 2001. Cytokines regulate the capacity of CD8alpha(+) and CD8alpha(−) dendritic cells to prime Th1/Th2 cells in vivo. *J. Immunol.* 167:4345–4350.

41. Maldonado-Lopez, R., and M. Moser. 2001. Dendritic cell subsets and the regulation of Th1/Th2 responses. *Semin. Immunol.* 13:275–282.

42. Brooks, D.G., L. Teyton, M.B. Oldstone, and D.B. McGavern. 2005. Intrinsic functional dysregulation of CD4 T cells occurs rapidly following persistent viral infection. *J. Virol.* 79:10514–10527.

43. Cao, W., M.D. Henry, P. Borrow, H. Yamada, J.H. Elder, E.V. Ravkov, S.T. Nichol, R.W. Compans, K.P. Campbell, and M.B. Oldstone. 1998. Identification of alpha-dystroglycan as a receptor for lymphocytic choriomeningitis virus and Lassa fever virus. *Science.* 282:2079–2081.

44. Brooks, D.G., M.J. Trifilo, K.H. Edelmann, H. Lewicki, L. Teyton, D.B. McGavern, and M.B.A. Oldstone. 2006. Interleukin-10 determines viral clearance or persistence in vivo. *Nat. Med.* In press.

45. Fiorentino, D.F., A. Zlotnik, P. Vieira, T.R. Mosmann, M. Howard, K.W. Moore, and A. O'Garra. 1991. IL-10 acts on the antigen-presenting cell to inhibit cytokine production by Th1 cells. *J. Immunol.* 146:3444–3451.

46. Liu, L., B.E. Rich, J. Inobe, W. Chen, and H.L. Weiner. 1998. Induction of Th2 cell differentiation in the primary immune response: dendritic cells isolated from adherent cell culture treated with IL-10 prime naive CD4+ T cells to secrete IL-4. *Int. Immunol.* 10:1017–1026.

47. Lin, M.Y., and R.M. Welsh. 1998. Stability and diversity of T cell receptor repertoire usage during lymphocytic choriomeningitis virus infection of mice. *J. Exp. Med.* 188:1993–2005.

48. Probst, H.C., and M. van den Broek. 2005. Priming of CTLs by lymphocytic choriomeningitis virus depends on dendritic cells. *J. Immunol.* 174:3920–3924.

49. Sevilla, N., S. Kunz, A. Holz, H. Lewicki, D. Homann, H. Yamada, K.P. Campbell, J.C. de La Torre, and M.B. Oldstone. 2000. Immunosuppression and resultant viral persistence by specific viral targeting of dendritic cells. *J. Exp. Med.* 192:1249–1260.

50. Liu, Y.J. 2001. Dendritic cell subsets and lineages, and their functions in innate and adaptive immunity. *Cell.* 106:259–262.

51. Pulendran, B., J.L. Smith, G. Caspary, K. Brasel, D. Pettit, E. Maraskovsky, and C.R. Maliszewski. 1999. Distinct dendritic cell subsets differentially regulate the class of immune response in vivo. *Proc. Natl. Acad. Sci. USA.* 96:1036–1041.

52. Oxenius, A., M.F. Bachmann, R.M. Zinkernagel, and H. Hengartner. 1998. Virus-specific MHC-class II-restricted TCR-transgenic mice: effects on humoral and cellular immune responses after viral infection. *Eur. J. Immunol.* 28:390–400.

53. Masopust, D., S.M. Kaech, E.J. Wherry, and R. Ahmed. 2004. The role of programming in memory T-cell development. *Curr. Opin. Immunol.* 16:217–225.

54. Re, F., and J.L. Strominger. 2001. Toll-like receptor 2 (TLR2) and TLR4 differentially activate human dendritic cells. *J. Biol. Chem.* 276:37692–37699.

55. Mosmann, T.R., H. Cherwinski, M.W. Bond, M.A. Giedlin, and R.L. Coffman. 1986. Two types of murine helper T cell clone. I. Definition according to profiles of lymphokine activities and secreted proteins. *J. Immunol.* 136:2348–2357.

56. Re, F., and J.L. Strominger. 2004. IL-10 released by concomitant TLR2 stimulation blocks the induction of a subset of Th1 cytokines that are specifically induced by TLR4 or TLR3 in human dendritic cells. *J. Immunol.* 173:7548–7555.

57. Lee, K.J., M. Perez, D.D. Pinschewer, and J.C. de la Torre. 2002. Identification of the lymphocytic choriomeningitis virus (LCMV) proteins required to rescue LCMV RNA analogs into LCMV-like particles. *J. Virol.* 76:6393–6397.

58. McFarland, H.I., S.R. Nahill, J.W. Maciaszek, and R.M. Welsh. 1992. CD11b (Mac-1): a marker for CD8+ cytotoxic T cell activation and memory in virus infection. *J. Immunol.* 149:1326–1333.

59. Lin, Y., T.J. Roberts, V. Sriram, S. Cho, and R.R. Brutkiewicz. 2003. Myeloid marker expression on antiviral CD8+ T cells following an acute virus infection. *Eur. J. Immunol.* 33:2736–2743.

60. Filippi, C., S. Hugues, J. Cazareth, V. Julia, N. Glaichenhaus, and S. Ugolini. 2003. CD4+ T cell polarization in mice is modulated by strain-specific major histocompatibility complex–independent differences within dendritic cells. *J. Exp. Med.* 198:201–209.

61. Liu, F., and J.L. Whitton. 2005. Cutting edge: re-evaluating the in vivo cytokine responses of CD8+ T cells during primary and secondary viral infections. *J. Immunol.* 174:5936–5940.